PARTS OF THE ORIGINAL DOCUMENT

ARE OF POOR REPRODUCTIVE QUALITY

CERTAINES PARTIES DU DOCUMENT ORIGINAL

SONT DE PIÈTRE QUALITÉ DE REPRODUCTION

CONTRACT SERIAL NO. OST84-00512
REQUISITION NO. 23440-5-9015
CONTRACTOR: QUEEN'S UNIVERSITY

PILOT SCALE TRIALS ON ATMOSPHERIC FLUIDIZED BED COMBUSTION OF A WESTERN CANADIAN SUB-BITUMINOUS COAL (HIGHVALE)

H.A. Becker, R.K. Code and J.R. Stephenson
Department of Chemical Engineering
Queen's University at Kingston
Kingston, Canada K7L 3N6

A report to
Energy Mines and Resources Canada
Energy Research Laboratories, CANMET
Ottawa, Canada

Technical Report QFBC.TR.87.3
Queen's Fluidized Bed Combustion Laboratory

41 pp

MICROMEDIA

ABSTRACT

Trials on the burning of a Western Canadian sub-bituminous coal (Highvale) were performed in an atmospheric fluidized bed combustion (AFBC) pilot plant (bed area 0.155 m^2). The conditions of the trials were mean coal particle diameter, 10.6 mm; fluidizing velocity, 1.1---3.1 m/s; excess air, -1.7---55 %; recycle ratio (fraction of cyclone catch recycled), 0---0.95; bed temperature, 750---950 °C. The bed was of sand, 0.6 mm mean particle diameter. The combustion efficiency as measured by carbon burn-up was 98---99.6% . An empirical correlation relates overhead carbon loss to the operating variables. Comparision with correlations obtained from trials on Eastern Canadian bituminous coals indicates that free swelling index is an important fuel characteristic affecting overhead carbon loss in AFBC systems. Since the bed was of sand, calcium entered only through the mineral matter of the coal. Because of its low sulphur and high shale contents, the coal by itself provided a high Ca/S mole ratio, 3.7. The observed sulphur capture was 80---99% while operating with underbed fuel injection and decreased to 50---95% with overbed fuel injection.

PREFACE.

This is the final report on one of the tasks performed under a contract with Supply and Services Canada (DSS) under the auspices of the Canada Center for Mineral and Energy Technology (CANMET), Energy, Mines and Resources Canada :

DSS Contract Serial No. : OST84-00512

Title : A Program of Pilot Scale R&D on Bubbling-Bed Atmospheric Fluidized Bed Combustion

Principal Investigators : Dr. H.A. Becker and Dr. R.K. Code, Department of Chemical Engineering, Queen's University at Kingston, Kingston, Ontario K7L 3N6, Telephone (613) 545-2767

Scientific Authority : Dr. E.J. Anthony, Building 1, Energy Research Laboratories, CANMET, Haanel Drive, Bells Corners, Ontario.
Postal address : Energy Research Laboratories, CANMET, 555 Booth Street, Ottawa, Ontario, K1A 0G1. Telephone (613) 996-4570, ext 185

Commencement date : April 1, 1985

Delivery date : March 31, 1987

Consignee : Energy, Mines and Resources, Energy Research Laboratories, CANMET, 555 Booth Street, Ottawa, Ontario K1A 0G1

Science Procurement Manager : Ms. J.P.S. Sztramko, Science Branch, Supply and Services Canada, Place du Portage, Phase III, 11 Laurier Street, Hull, Quebec K1A 0D5

CONTENTS

NOTATION 5

1. INTRODUCTION 7

2. THE PILOT PLANT 7

3. MATERIALS 8

4. OPERATING CONDITIONS 11

5. THE CARBON BALANCE 16

5.1 Carbon content of solids 16
5.2 Flux distribution 18
5.3 Carbon burn-up inefficiency 20

6. THE SULPHUR BALANCE 27

7. THE NITROGEN BALANCE 28

8. CARBON MONOXIDE 30

9. COMPARISION WITH OTHER COALS 31

9.1 Overhead carbon loss 31
9.2 Sulphur capture 33

10. COMPARISION WITH ERL TRIALS ON HIGHVALE COAL 34

10.1 Background 34
10.2 Overhead carbon loss 34
10.3 Sulphur capture 36

11. CONCLUSIONS 38

REFERENCES.....39

TABLES

3.1 Chemical analysis of Highvale coal, nominal size -1 inch.10
3.2 Particle size distributions of the materials.....11
4.1 Operating conditions 14
5.1 Statistical data on the overhead carbon loss correlation.24
9.1 Correlation of overhead carbon loss for the temperature range 800---950°C.....31

FIGURES

2.1 Schematic representation of the AFBC pilot plant.....9
3.1 Particle size distribution of Kingston sand.....12
3.2 Particle size distribution of Highvale coal.....13
4.1 Oxygen content of exhaust gas versus excess air level....15
5.1 Carbon content of solid products versus bed temperature..17
5.2 Flux ratio of carbon loss in solids to carbon fed in the fuel versus bed temperature.....19
5.3 Carbon burn-up efficiency versus bed temperature.....20
5.4 Flux ratio of carbon loss in the bed product stream to carbon fed in the fuel versus bed product flow rate.....21
5.5 Flux ratio of overhead carbon loss to carbon fed in the fuel versus bed temperature.....22
5.6 Effect of bed temperature on overhead carbon loss.....25
5.7 Overhead carbon loss predicted by empirical correlation versus overhead carbon loss measured.....26
6.1 Sulphur capture efficiency based on gas analysis as a function of bed temperature.....27
7.1 THe NOX content of the exhaust gases as a function of oxygen concentration.....28
7.2 Fraction of fuel nitrogen converted to NOX versus bed temperature.....29
7.3 Fraction of fuel nitrogen converted to NOX versus the elutriated carbon flux.....29
7.4 Fraction of fuel nitrogen converted to NOX as a function of stack gas oxygen concentration.....30
8.1 Carbon monoxide content of the exhaust gases versus oxygen content.....30

FIGURES cont'd

9.1 Flux ratio of overhead carbon loss to carbon fed in the fuel predicted by empirical correlation versus fuel free swelling index.....32

10.1 Flux ratio of overhead carbon loss to carbon fed in the fuel as a function of bed temperature.....35

10.2 Sulphur capture efficiency versus bed temperature.....37

NOTATION

Subscripts (codes for material streams)

a	combustion air
b	bed product (material removed directly from the bed)
c	cyclone product (cyclone catch not recycled)
d	cycloned solids (dust catch in cyclone; equals recycled cyclone solids r plus cyclone product p)
e	elutriated solids (cycloned solids d plus baghouse product h)
f	fuel (here coal)
g	stack gas
h	baghouse product
o	overhead product solids (cyclone product c plus baghouse product h)
p	total product solids
r	recycled cycloned solids
s	sorbent or bed material (here sand)

Variables

COT	continuous-mode operating time, h
D_p	particle diameter, mm. Here determined by sieve analysis
$\hat{D}_p$	characteristic diameter for particles of mixed size, mm : defined by $\hat{D}_p = D_p$ at $F_D = 1/2$
F_D	distribution function, $F_D = F_D(D_p)$, of particle size in a population : the mass fraction of particles smaller than the argument value of D_p
FSI	free swelling index of coal
m	mass of material, kg
m_b	bed mass (holdup), kg
$\dot{m}$	mass flux, kg/h
n_t	number of in-bed cooling tubes
r	recycle fraction; fraction of cycloned dust that is returned to the combustor

NOTATION cont'd

T_b	bed temperature, K
v	superficial gas velocity up the combustor, m/s, also called the fluidizing velocity ; measured at the bed temperature, freeboard pressure, and exit gas compositions
$W_{i,m}$	mass ratio of component i in the m'th material stream, here the mass fraction d.b. (dry basis), i.e., the mass fraction of i per unit mass of dry matter
ε_a	excess air level, $\dot{n}_a/\dot{n}_{a,st} - 1$, where $\dot{n}_{a,st}$ is the theoretical air requirement for complete combustion, also expressed as a percentage
τ_b	$= m_b/\dot{m}_b$, estimate of residence time of bed product in combustor, h
τ_p	$= m_b/\dot{m}_p$, mean residence time of particles in combustor, h
ϕ_a	air equivalence ratio: $1 + \varepsilon_a$
$\phi_{i,mn}$	mass flux ratio of component i in the m'th and n'th material streams

Acronyms

AFBC	atmospheric fluidized bed combustion
ASTM	American Society for Testing Materials
CBE	carbon burn-up efficiency
ERL	Energy Research Laboratories, CANMET, Energy Mines and Resources Canada
MAF	moisture and ash free basis
SCE	sulphur capture efficiency
QFBC	Queen's Fluidized Bed Combustion Laboratory
OCLO	overhead carbon loss observed
OCLP	overhead carbon loss predicted

1. Introduction

The present work is another in a series of investigations of the burning of Canadian candidate fuels by atmospheric fluidized bed combustion (AFBC). The fuels examined in previous studies (Becker and Code 1983; Becker Code McCleave and Stephenson 1985) were Eastern Canadian coals (Minto, Devco, Evans), an Appalachian coal (Kentucky no. 9), and Syncrude coke. The objectives set for the present study were :

1. Conduct combustion trials with a Western sub-bituminous coal, Highvale, using a test matrix suitable for allowing comparision with the performance of the previously studied Eastern Canadian fuels and with published results on the AFBC performance of Highvale coal (Stover et al, 1981)

2. Investigate the effects of overbed versus underbed fuel injection

3. Determine combustion efficiency as indicated by carbon burn-up

4. Determine the sulphur capture by the fuel ash, which is high in calcium

5. Determine the extent of fuel nitrogen conversion to NO_x

2. The pilot plant

The pilot plant, schematically illustrated in Figure 2.1 is described in detail elsewhere (Becker and Code 1982). The combustion chamber is square in cross-section, 0.155 m^2 in area. The height from air distributor to top of freeboard is 4 m . Up to 48 in-bed cooling tubes can be inserted to absorb heat from

the bed. Elutriated fines are largely caught by a cyclone separator, and nearly all the rest are captured in a baghouse.

3. Materials

Highvale coal is surfaced-mined in central Alberta to fuel the Sundance thermal generation station. It is ranked as sub-bituminous (ASTM classification) and is non-caking, having a free swelling index of zero. Analytical data for this fuel is summarized in Table 3.1. There are four major differences between Highvale coal and the eastern Canadian coals previously studied (Minto, Devco and Evans), that would tend to enhance AFBC performance. They are :

- low sulphur content
- high calcium content
- low free swelling index
- high ash fusion temperatures

The natural Ca/S mole ratio of the coal as received was 3.7. The use of limestone to capture sulphur dioxide was therefore ruled out for this reason as well as for the fact that coal of such low sulphur content, 0.3 %, would not under present regulations require SO_2 emmision control in combustion applications. If the coal were crushed to a suitably small size, around 0.5---3 mm mean diameter, then the shaley portion of the coal ash might be utilized as the stable bed material. This option, requring very large run times and coal consumption to establish the bed, was not explored. Instead, a sand bed was used in all the trials. The sand, a double screened product designed for applications in sand blasting, was obtained locally.

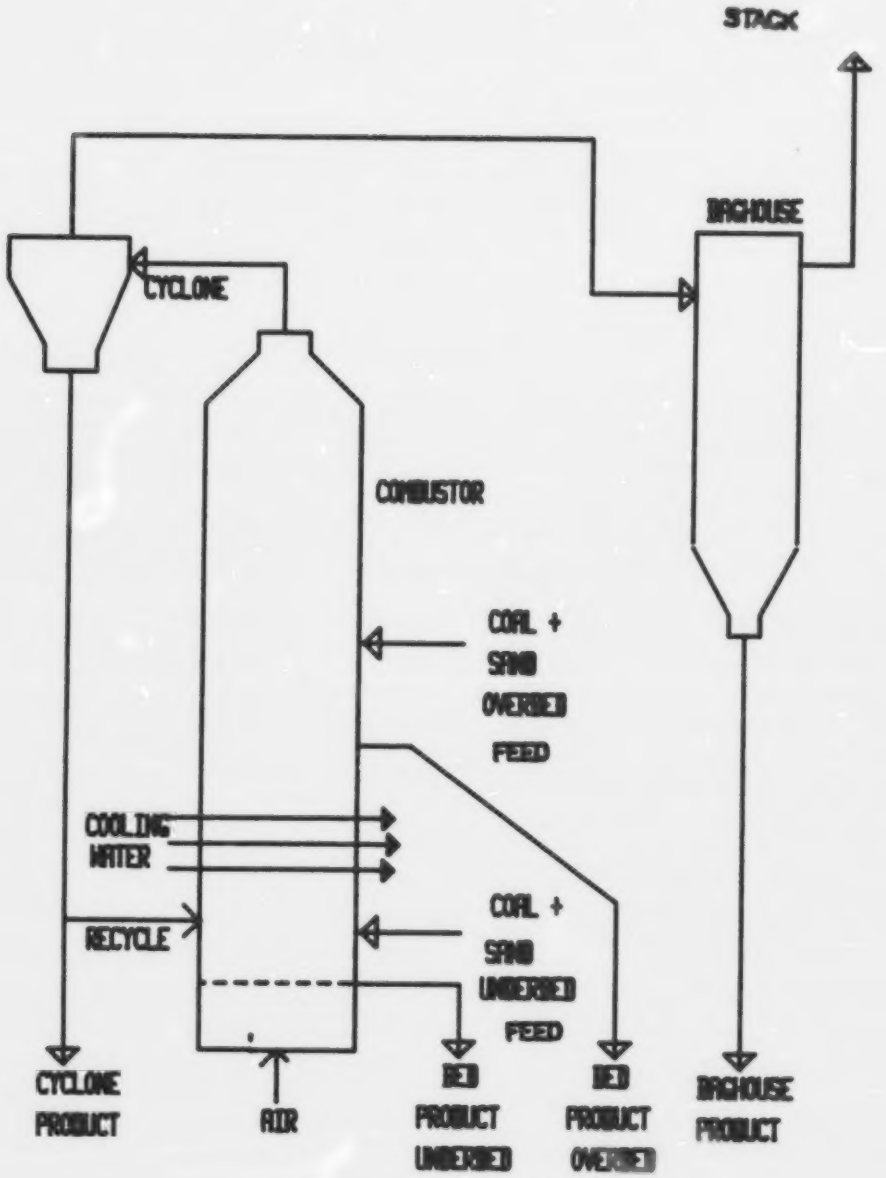

Fig. 2.1 Schematic representation of the AFBC pilot plant.

Table 3.1 Chemical analysis of Highvale coal, nominal size -1 inch.

Proximate/Ultimate Analysis

(weight %, dry basis)

Reporter	QFBC[a]	ERL[b]	Stover[c]
MOIS	17.99	12.69	13-19
ASH	16.85	15.13	16.02
VCM	33.21	33.46	33.71
FC	49.81	51.41	50.27
C	61.31	64.95	63.54
H	3.82	3.64	2.54
N	0.63	0.76	0.78
S	0.31	0.32	0.24
O	17.26	15.20	16.88

Sulfur Forms[c]

(weight %, dry basis)

Pyritic	0.05
Sulphatic	0.00
Organic	0.19
Total	0.24

Ash Analysis

(weight %, ignited basis)

Reporter	QFBC[a]	ERL[b]	Stover[c]
SiO_2		48.13	52.71
AL_2O_3		20.78	23.08
Fe_2O_3		4.49	4.77
TiO_2		0.74	0.68
CaO		11.94	11.32
MgO		1.15	1.31
Na_2O		2.92	2.66
K_2O		0.36	0.35
BaO		0.38	
SrO		0.10	
SO_3	2.72	6.38	3.08
Mn_3O_4			
P_2O_4			0.43

Calorific Value

(MJ/kg, MAF)

QFBC[a]	ERL[b]	Stover[c]
26.41	28.22	28.95

[a] Present lot of coal, average analysis of 6 samples.

[b] Anthony (1986), analysis of single sample from present lot.

[c] Stover et al (1981)

The particle size distributions of the coal and sand feed materials are summarized in Table 3.2 and illustrated graphically in Figures 3.1 and 3.2.

Table 3.2 Particle size distributions of the materials.

Material	Fraction by mass undersize, F_D					
	0.02	0.10	0.20	0.50	0.80	0.95
	D_p by sieve analysis, mm					
Highvale	0.09	1.51	4.41	10.8	16.7	21.6
Sand	0.01	0.19	0.30	0.60	0.86	1.14

Shale particles comprise a portion of the mineral component of Highvale coal. Because of the large top size of the fuel, and similar top size of the associated shale particles, a stagnant layer of unfluidizable particles tended to accumulate during operation.

4. Operating conditions

The operating conditions of the fifteen Highvale trials are summarized in Table 4.1. The earlier work of Stover et al (1981) on Highvale coal indicated bed temperature to be the most important variable controlling overhead carbon loss. In order to allow direct comparisons between the rigs, this variable was set at the same levels they used.

The range of superficial fluidizing velocity covered in the present work was 1.1---3.1 m/s . The lower limit represents operation at a reasonable through-put, well above minimum fluidizing velocity. The large top size of the fuel (one inch) imposed spacing requirements on the in-bed cooling tubes,

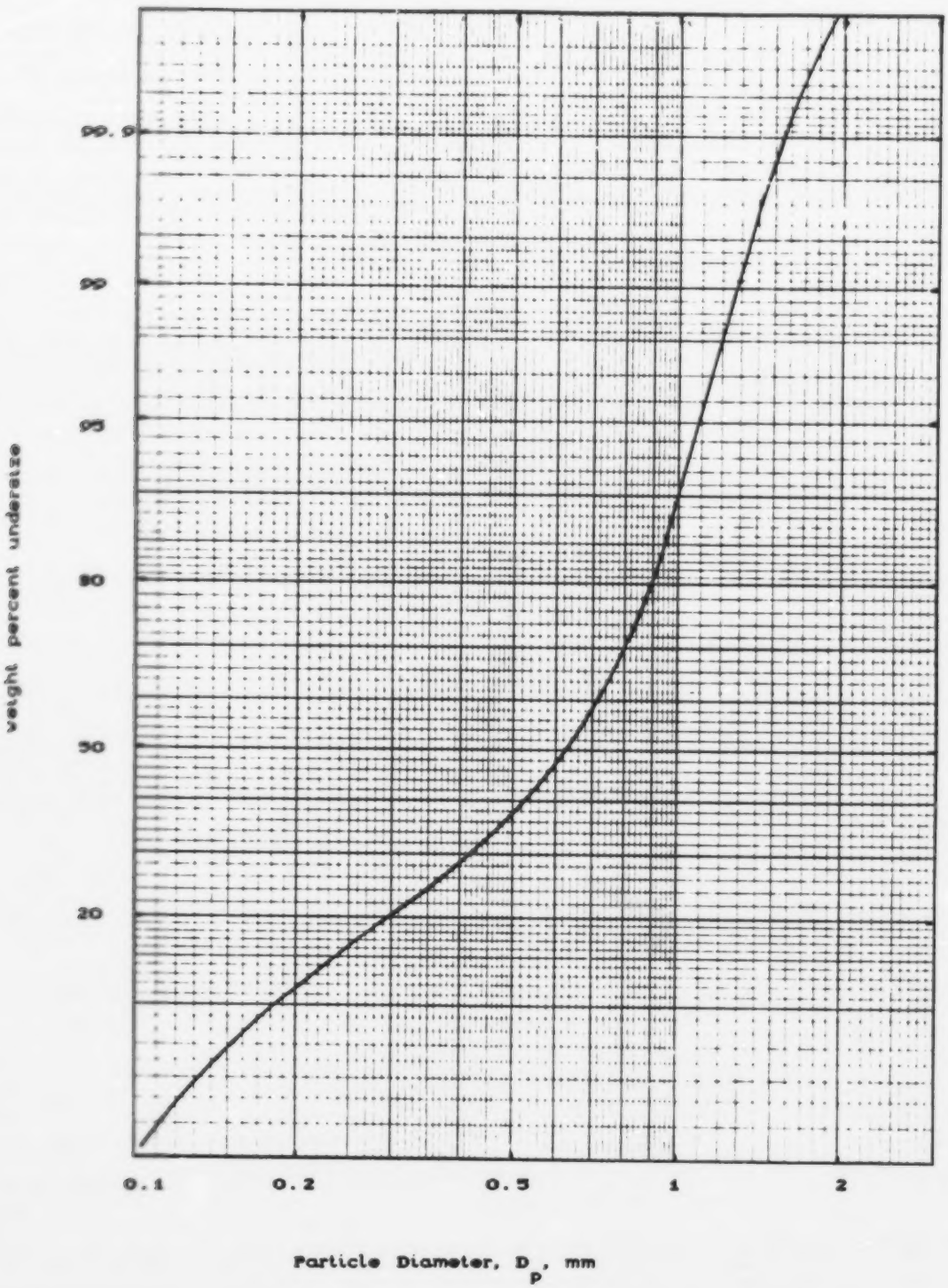

Fig. 3.1 Particle size distribution of Kingston sand.

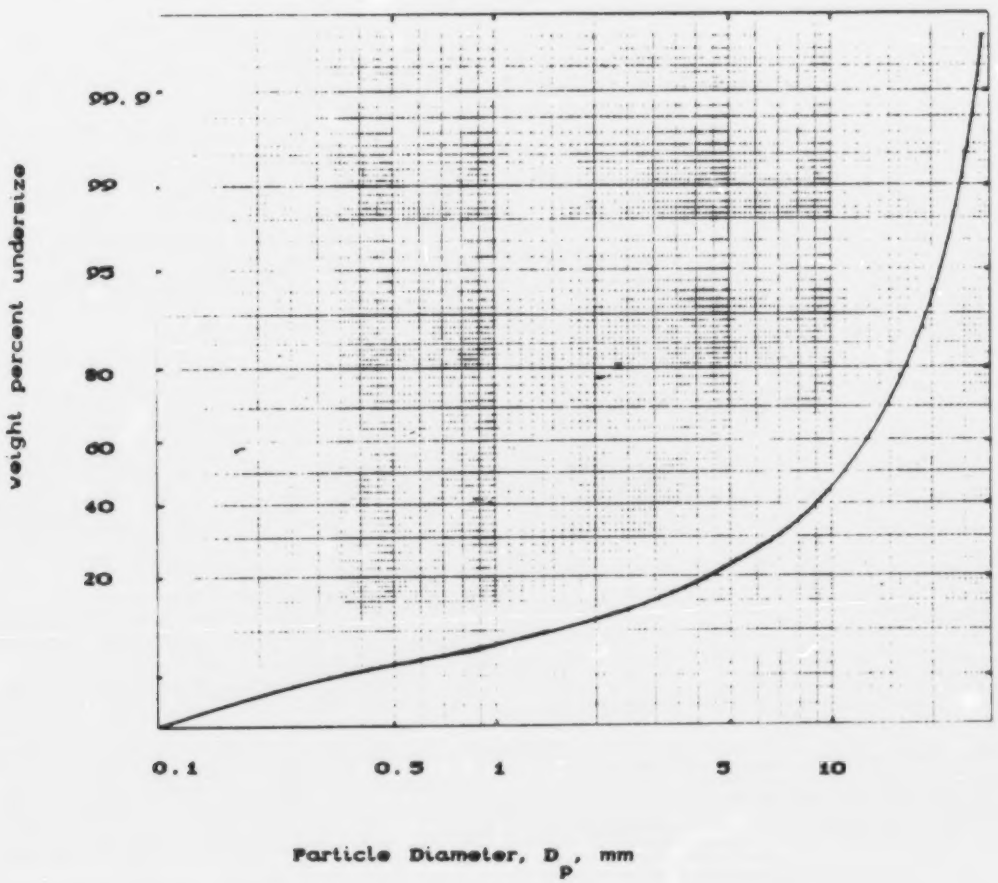

Fig. 3.2 Particle size distribution of Highvale coal.

Table 4.1 Operating conditions.

Trial	n_t	Fuel		SAND		Ca/S	Air		r	T_b, °C	v, m/s	τ_p, h	τ_b, h	COT, h
		D_p, mm	$\dot{m}_f$, kg/h	D_p, mm	$\dot{m}_s$, kg/h		$\dot{m}_a$, kg/h	ϵ_a, %						
		HIGHVALE												
860507	6	10.8	26.1	0.6	4.6	0	221	31.3	0.00	751	1.1	15.0	41.0	8.0
860416	16	10.8	41.8	0.6	3.9	0	334	23.7	0.93	749	1.7	11.3	18.0	8.0
860415	16	10.8	42.1	0.6	4.6	0	365	34.1	0.00	751	1.9	9.0	22.2	8.5
860501*	16	10.8	40.4	0.6	4.9	0	336	28.8	0.00	749	1.7	10.9	28.3	8.0
860502*	16	10.8	44.2	0.6	5.0	0	355	24.5	0.95	749	1.8	10.8	15.5	6.0
860418	16	10.8	41.6	0.6	3.6	0	326	21.1	0.00	798	1.8	10.8	31.3	5.0
860508	6	10.8	30.8	0.6	3.6	0	255	28.1	0.00	851	1.5	10.3	18.5	8.0
860409	8	10.8	37.6	0.6	5.4	0	239	-1.7	0.00	847	1.4	13.4	54.4	10.0
860408	8	10.8	38.1	0.6	4.5	0	384	54.6	0.00	847	2.2	11.5	39.4	10.0
860417	16	10.8	50.7	0.6	4.1	0	406	23.8	0.00	850	2.3	7.7	21.8	8.0
860429*	16	10.8	54.3	0.6	4.9	0	419	19.6	0.00	851	2.4	8.5	22.5	8.0
860509	2	10.8	27.1	0.6	6.0	0	191	9.5	0.00	952	1.2	12.0	16.3	8.0
860510	2	10.8	27.3	0.6	3.6	0	239	35.2	0.00	950	1.5	13.3	20.6	6.0
860407	8	10.8	51.1	0.6	5.2	0	431	30.4	0.00	951	2.7	6.9	20.4	10.0
860430*	16	10.8	67.6	0.6	4.2	0	504	15.5	0.00	954	3.1	5.4	13.1	5.0

* - overbed feed, underbed ash extraction
others - underbed feed, overbed ash extraction

limiting their number to sixteen. This limited the upper bound of the fluidizing velocity and imposed a correlation with bed temperature.

The excess air level in the present work, Figure 4.1, covered a wide range, -2 to 55 %. This variable was not changed substantially for the low temperature trials ($T_b \cong 750^{\circ}C$), in order to clearly show the effect of cyclone product recycle at a bed temperature level where the previous work (Stover et al, 1981) indicated high overhead carbon loss. Because of the high combustion efficiencies obtained, the exhaust gas oxygen levels, Fig 4.1, were highly correlated with the excess air level.

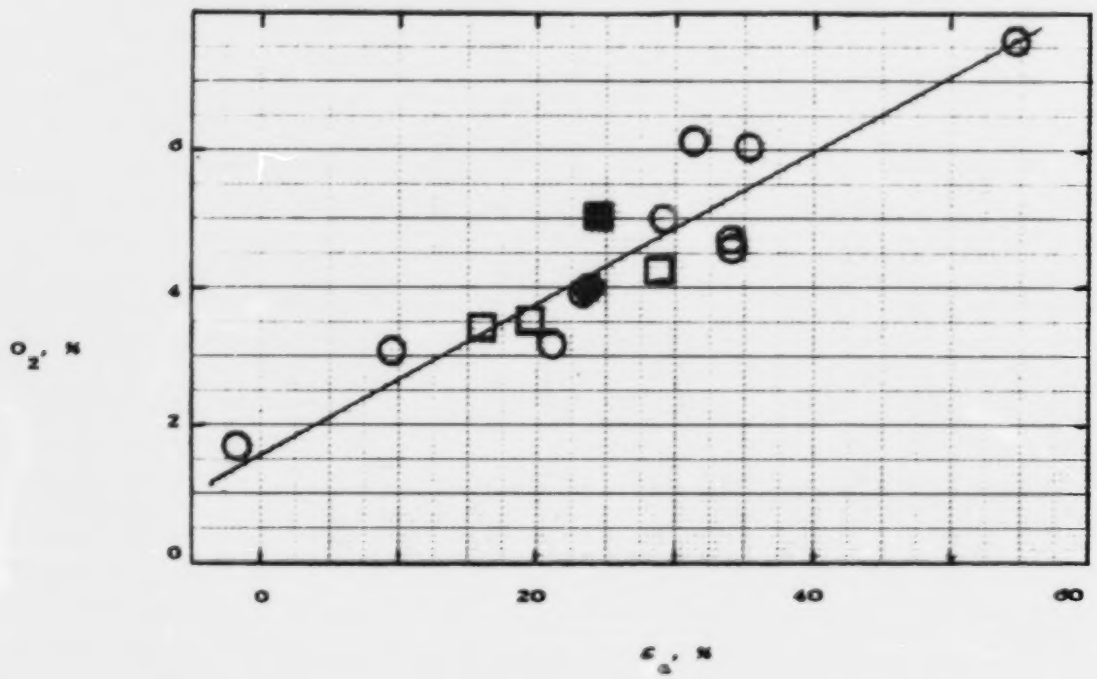

Fig. 4.1 Oxygen content of exhaust gas versus excess air level.
key to symbols :

- ● ○ - underbed feed, overbed extraction
- ■ □ - overbed feed, underbed extraction
- ○ □ - r = 0
- ● ■ - r = 0.95---0.95

As part of a multi-fuel study, both overbed and underbed feed modes were used in the present work. To avoid short-circuiting of the fuel, underbed ash extraction was used in conjunction with overbed feeding, and overbed ash extraction with underbed feeding.

The range of expanded bed depth, as indicated by the wall pressure distribution, was 0.4---0.6 m. While operating in the overbed ash extraction mode, bed depth was regulated by ash overflow from a port located 1.2 m above the air distributor plate. While operating in the underbed ash extraction mode, bed product removal rates were regulated to maintain the expanded bed depth within the above range.

5. The carbon balance

5.1 Carbon content of solids

Figure 5.1 shows the carbon content of the product streams as a function of bed temperature. The ranges of carbon content are : 0.4---2.6 % for the bed product, 0.5---8 % for the cyclone product, and 2---27 % for the baghouse product. For the bed product stream, there is a clear effect of reduction in carbon content with increasing bed temperature . The effect of changing ash removal points from overbed to underbed is small, indicating good vertical mixing of the fuel in the bed.

Trends in the carbon content of the cyclone and baghouse streams are masked by the varying inert sand content in these materials. This effect is removed by examination of the carbon flux in the next section.

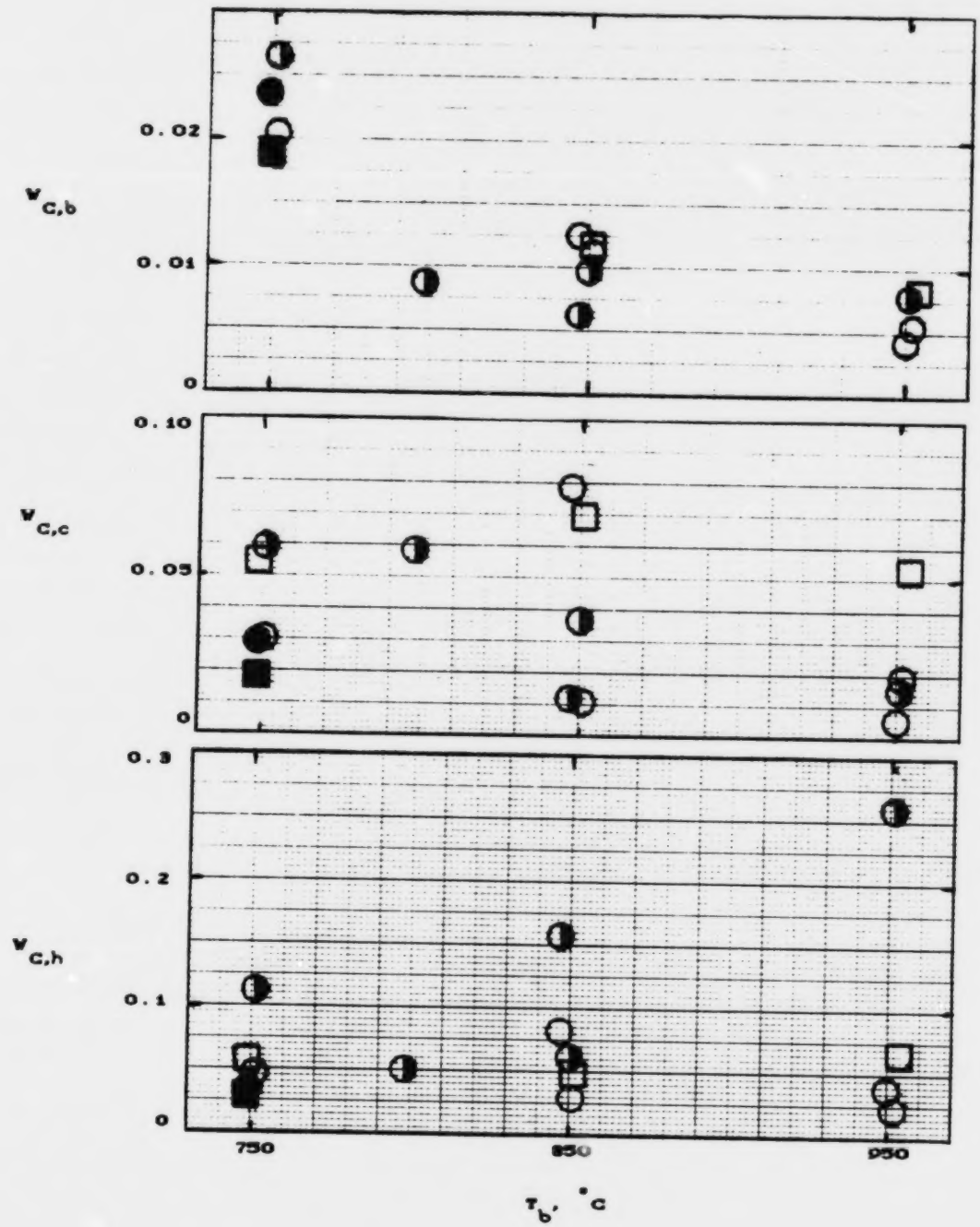

Fig. 5.1 Carbon content of solid products versus bed temperature.

Key to symbols:

○ - underbed feed; v = 1.1---1.5 m/s; r = 0
◑ - underbed feed; v = 1.6---3.1 m/s; r = 0
● - underbed feed; v = 1.6---3.1 m/s; r = 0.98
□ - overbed feed ; v = 1.6---3.1 m/s; r = 0
■ - overbed feed ; v = 1.6---3.1 m/s; r = 0.95

5.2 Flux distribution

Figure 5.2 shows the flux ratio of carbon carried in a given solids stream to carbon in the feed as a function of bed temperature. The ranges of these flux ratios are : 0.001---0.005 for the bed product,0.001---0.013 for the cyclone product, and 0.0004---0.006 for the baghouse product.

The flux ratio of carbon carried in the bed product stream to carbon in the feed ($\phi_{C,bf}$) is small, but not insignificant in comparison to the flux ratios of the other solid waste streams. As with the bed product carbon content, $\phi_{C,bf}$ tends to decrease with increasing bed temperature. The effect is less evident due to increased convective carbon loss, at a given temperature level, with increased bed product flow rate.

The flux ratios of carbon carried in the cyclone and baghouse product streams to the carbon in the feed ($\phi_{C,cf}$ & $\phi_{C,hf}$ respectively) tend to increase with increasing fluidizing velocity and decrease with increasing bed temperature.

Fines recycle at the 750 °C bed temperature level dramatically reduced $\phi_{C,cf}$ without large concurrent carbon load increases in the other solid waste streams.

The effect of feed injection point on $\phi_{C,bf}$ and $\phi_{C,cf}$ is negligible. However, when compared to runs of similar fluidizing velocity at a given temperature level, $\phi_{C,hf}$ was generally lower for the overbed feed trials. The reason for this unexpected result remains unclear, but will be examined in a separate report on the aforementioned multi-fuel study pertaining to the effects of fuel injection point.

The effect of excess air level cannot be clearly demonstrated in this data set because of concurrent changes in the other process variables. The effects of this variable are examined statistically in the next section.

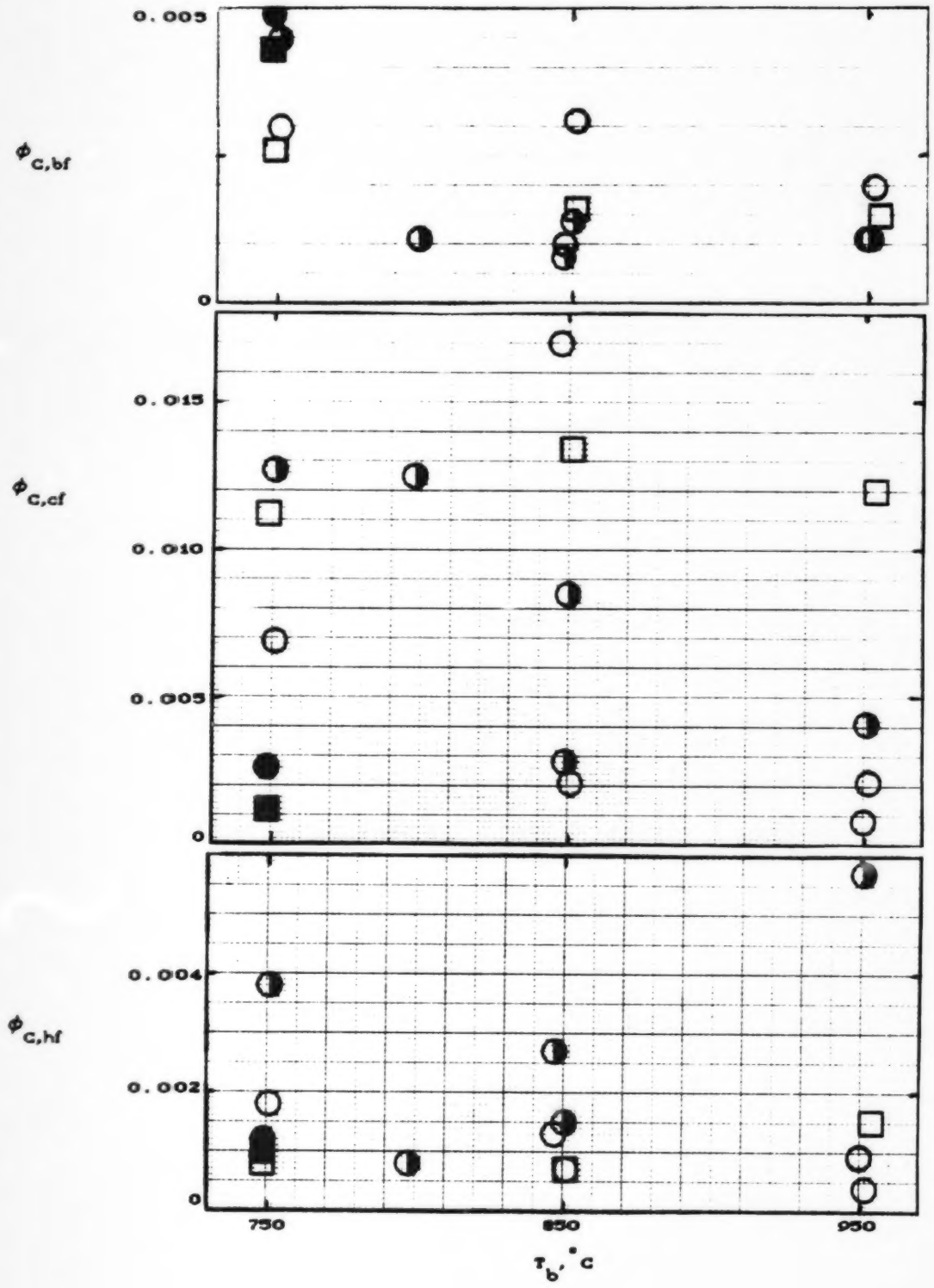

Fig. 5.2 Flux ratio of carbon loss in solids to carbon fed in the fuel versus bed temperature. Key to symbols in Fig 5.1.

5.3 Carbon burn-up inefficiency

Because of the small fuel hydrogen content in the product solid streams, combustion efficiency is closely related to the carbon burn-up efficiency (CBE). The CBE (plotted versus T_b in Figure 5.3) was generally quite high for the present set of trials, falling in the range 97.9---99.8 % .

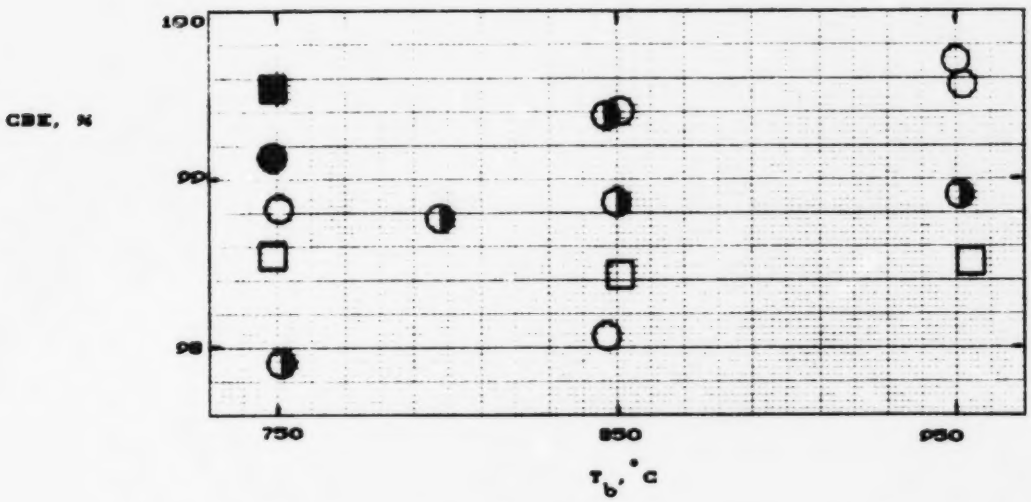

Fig. 5.3 Carbon burn-up efficiency versus bed temperature. Key to symbols in Fig 5.1

The total carbon combustion inefficiency can be usefully divided into two components, overhead carbon loss and bed product carbon loss ($\phi_{C,of}$ and $\phi_{C,bf}$, respectively).

Figure 5.4 shows $\phi_{C,bf}$ as a function of bed product flow rate. Clearly, the carbon burn-up inefficiency contribution from this product stream can be minimized by operating at bed temperatures greater than 800 °C and removing bed material at a rate no greater than that required for removing the defluidized

portion of the shale. The rate of shale accumulation in the bed was found to be approximately 3 % of the coal flow rate.

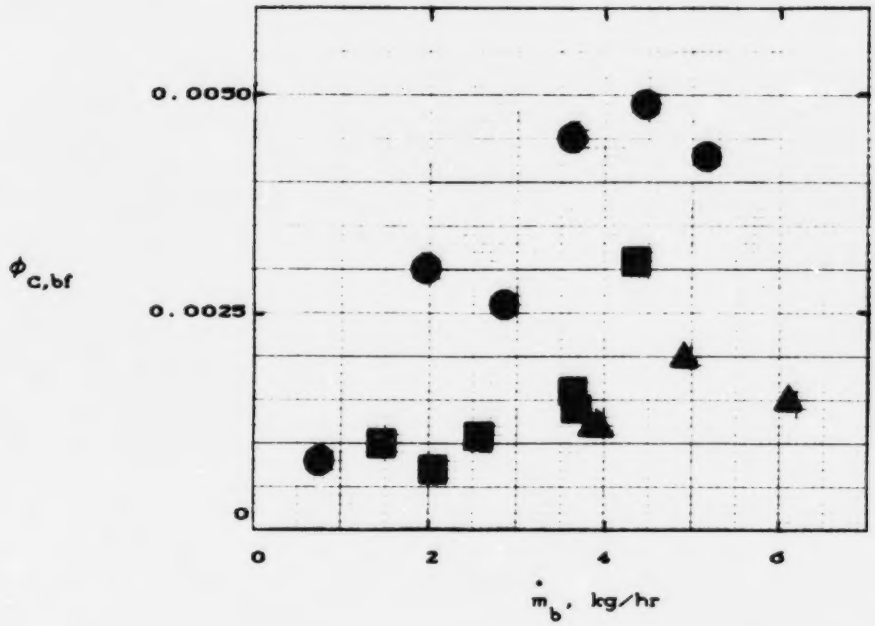

Fig. 5.4 Flux ratio of carbon loss in the bed product stream to carbon in the fuel versus bed product flow rate.

Key to symbols :

● - $T_b \cong 750$ °C
■ - T_b = 789---850 °C
▲ - $T_b \cong 950$ °C

The $\phi_{C,of}$ is shown in Figure 5.5 as a function of bed temperature. The expected trends with respect to temperature, fluidizing velocity, and cyclone product recycle are evident.

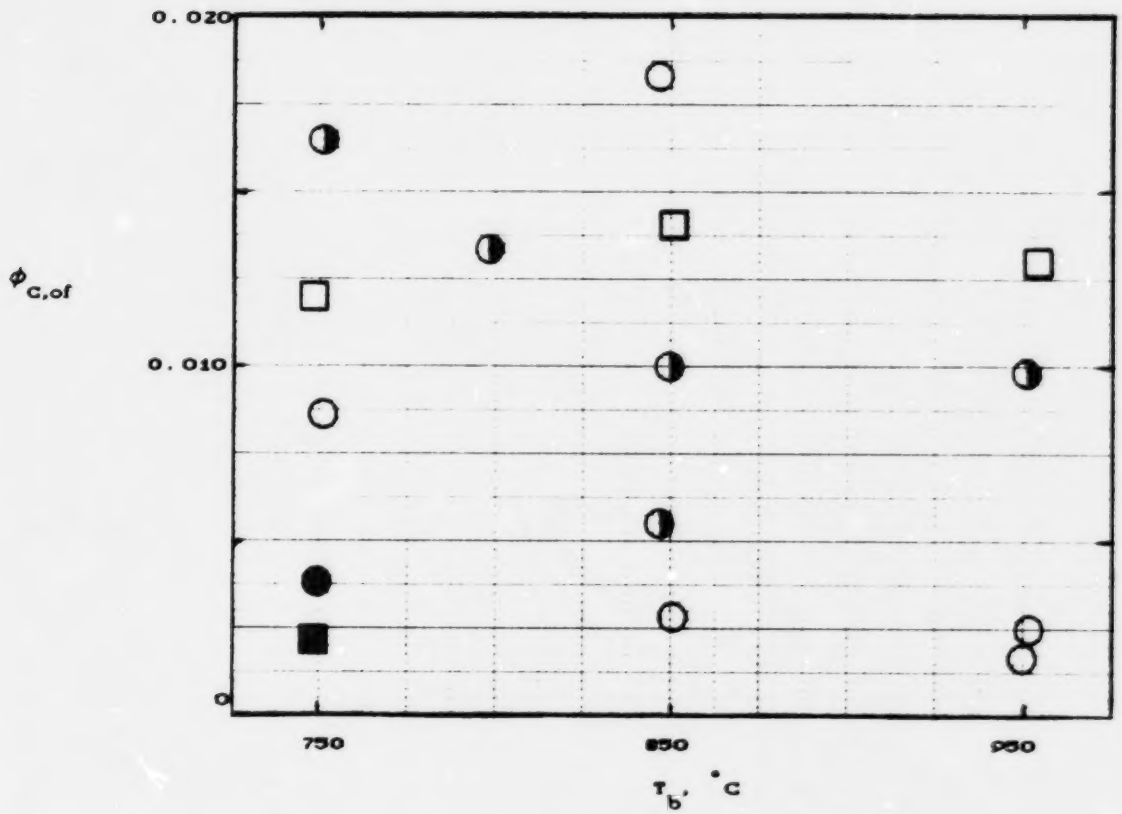

Fig. 5.5 Flux ratio of overhead carbon loss to carbon fed in fuel versus bed temperature. Key to symbols in Fig 5.1.

In our earlier work (Becker et al 1983 & 1985) on eastern Canadian coals (Minto, Devco and Evans), an empirical correlation for overhead carbon loss was developed of the form :

$$\ln \phi_{C,of} = a_o + a_1 \ln v + a_2 \ln \phi_a + a_3 r + a_4/T_b + a_5 \ln \hat{D}_{p,s} \quad (1)$$

where $\phi_a = 1 + \varepsilon_a$ is the mixture strength of Stover et al and T_b is the absolute bed temperature. Equation (1) can be written in the power law form:

$$\phi_{C,of} = C_o \; v^{a_1} \; \phi_a^{a_2} \; e^{(a_3 r)} \; e^{(a_4/T_b)} \; \hat{D}_{p,s}^{a_5} \quad (2)$$

where $C_o = \ln a_o$.

The sorbent particle diameter was not varied in the present work. Fitting the data to the remaining operating variables gave the following result :

$$\phi_{C,of} = 5.33 \times 10^{-7} \; v^{1.9} \; \phi_a^{-4.2.} \; e^{(-2.0r)} \; e^{(10500/T_b)} \quad (3)$$

The coefficents show the expected qualitative behaviour; increasing overhead carbon loss with increasing superficial fluidizing velocity, and decreasing overhead carbon loss with increasing excess air, fines recycle and bed temperature. Details on the multiple linear regression analysis are given in Table 5.1.

Table 5.1 Statistical data on the overhead carbon loss correlation, linear form of equation (3) .

Variable		Coefficients		
Symbol	Units	Symbol	Estimate	Std Error
v	m/s	a_1	1.9	0.32
ϕ_a	0	a_2	-4.2	0.88
r	0	a_3	-2.0	0.3
T_b	K	a_4	10500	1600
constant	0	a_0	-14.4	1.5

Standard error in estimate of $\ln(\phi_{C,of})$: 6.4 %
Multiple correlation coefficient : 0.88
F-ratio : 22

To clearly illustrate the effect of bed temperature on overhead carbon loss, a plot of $\phi_{C,of}/(v^{1.9}\ \phi_a^{-4.2}\ \exp(-2.0\ r))$ versus $1/T_b$ is shown in Figure 5.6 .

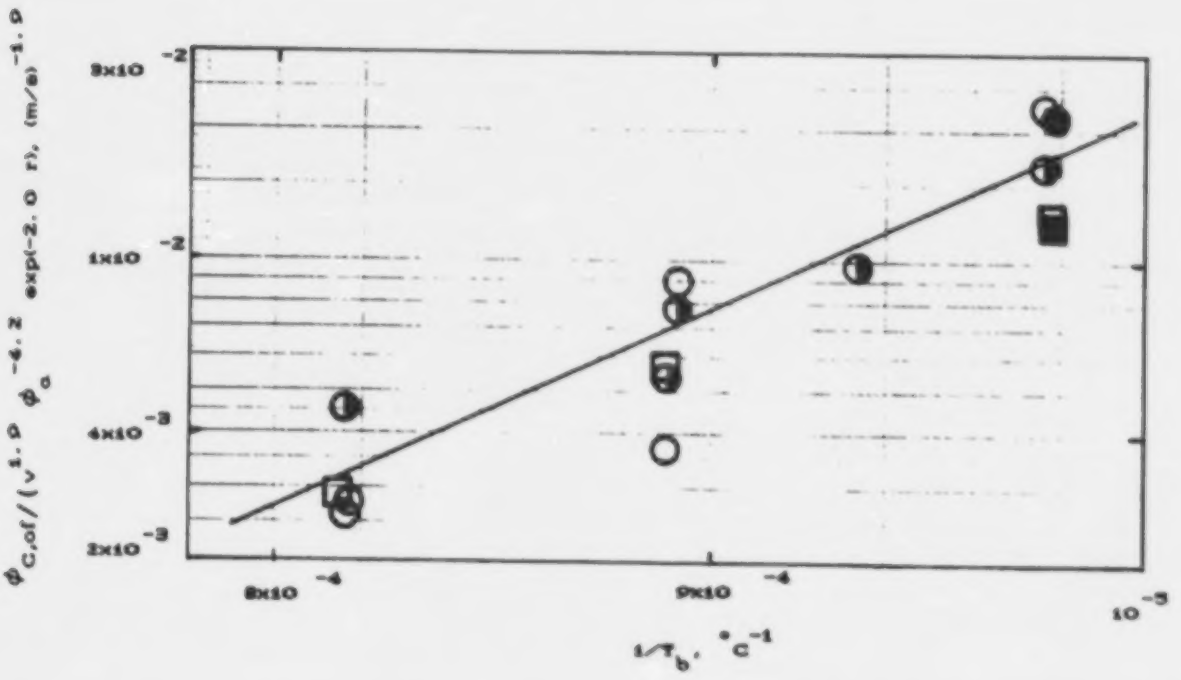

Fig 5.6 Effect of bed temperature on overhead carbon loss.
Key to symbols in Fig. 5.1.

Figure 5.7 shows the overhead carbon loss predicted by equation (3) versus the overhead carbon loss observed. The predicted values for the overbed feed trials are generally high. Since the effect is quite modest, it may be an artifact of this small data set.

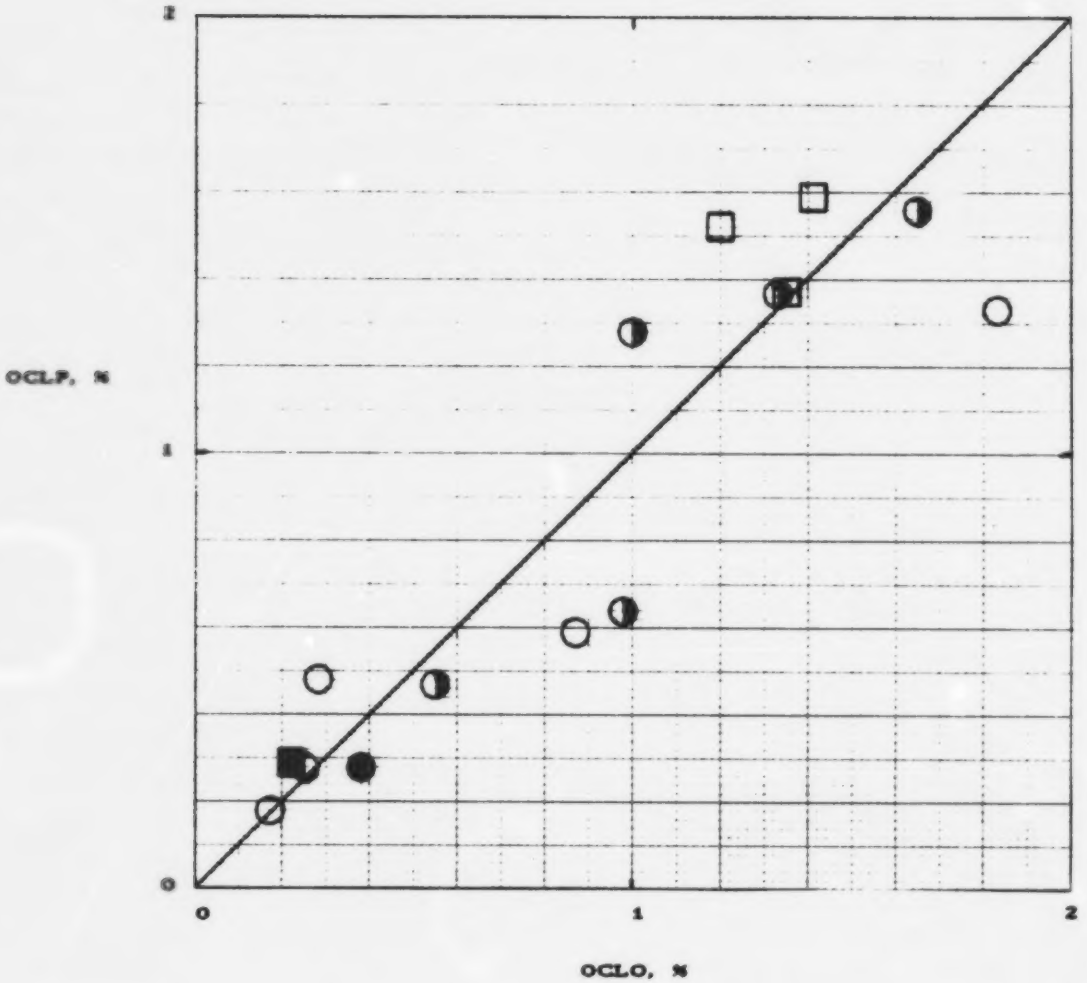

Fig 5.7 Overhead carbon loss predicted by empirical correlation versus the overhead carbon loss measured.
Key to symbols in Fig. 5.1.

6. The sulphur balance

The calcium to sulphur ratio for the present trials was fixed at 3.7, both elements being natural components of the fuel. Figure 6.1 shows the sulphur capture (calculated from the SO_2 emissions) as a function of bed temperature. The data from the underbed feed trials generally fall in the range 80---100 % and indicate a flat response to bed temperature. One point showing only 32 % sulphur capture is probably in error. Carbon monoxide levels were exceptionaly high during this trial, and may have interfered with the SO_2 measurement.

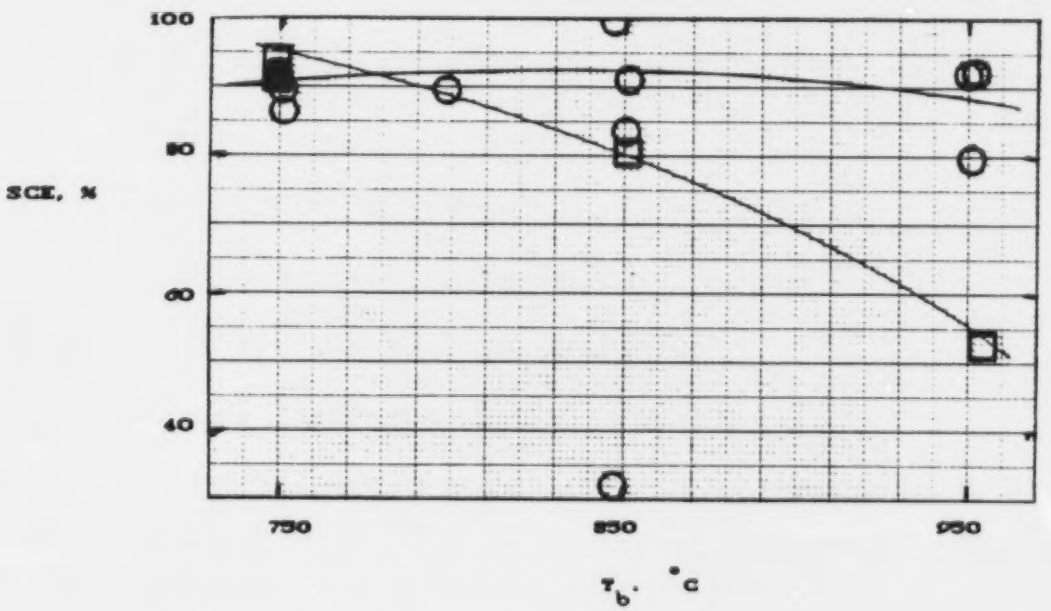

Fig 6.1 Sulphur capture efficiency based on gas analysis as a function of bed temperature. Key to symbols in Fig. 4.1.

The data from the overbed feed trials fall in the 50---95 % sulphur capture range, and show a strong decrease in capture with increasing bed temperature. This effect may be explained in the following manner. As bed temperature is increased, the proportion of sulphur released from a fuel particle before effective submersion in the bed increases. The

sulphur so released into the freeboard does not effectively contact the calcium-rich shale particles which are concentrated in the bed, so the overall sulphur capture is reduced, thereby reducing the overall sulphur capture efficency.

The sulphur balances for these trials were poor, leaving 30 to 65 % of the sulphur unaccounted for. Because of the low bed ash flow rates, the usual condition for steady-state operation (operating times of at least two bed turnovers) was unattainable. The reduced population of shale particles in the bed prior to steady-state, and hence in the ash product stream, probably caused the large sulphur balance error.

7. The nitrogen balance

Due to an instrument failure, NO_x emission data were not obtained for nine of the runs. Figure 7.1 shows the exhaust gas NO_x concentration as a function of exhaust O_2 concentration for the others. A strong correlation is evident and the results agree with the general observation that NO_x emission is minimized by keeping the exhaust O_2 level low.

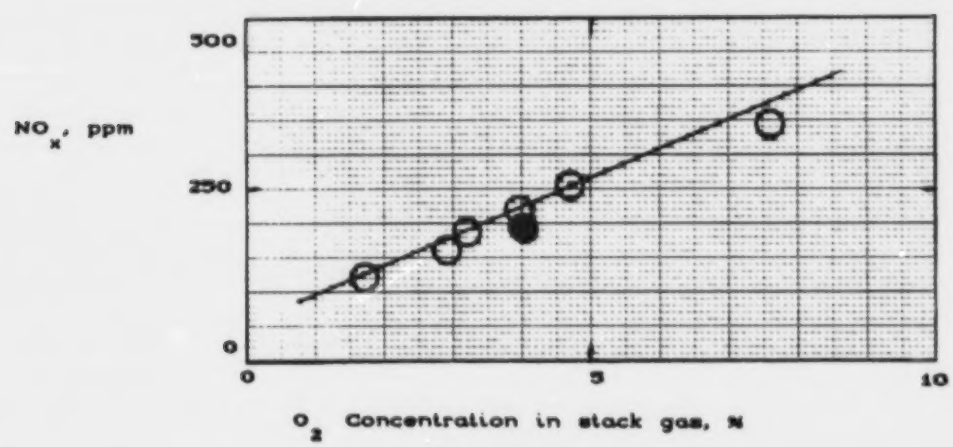

Fig. 7.1 The NO_x content of the exhaust gases as a function of oxygen concentration. Key to symbols in Fig. 4.1.

The proportion of fuel nitrogen converted to NO_x ($\phi_{N,gf}$) is shown in Figures 7.2 to 7.4 as a function of exhaust O_2 concentration, mass flow rate of elutriated carbon, and bed temperature. The only strong trend is that of increasing $\phi_{N,gf}$ with increasing exhaust O_2 concentration. The range of $\phi_{N,gf}$, 0.1---0.4, is somewhat higher than that observed with other fuels, typically 0.1---0.25 (Becker et al, 1985). This may be a consequence of the relatively low mass flow rate of elutriated carbon observed in the present trials, significantly lowering freeboard char concentration levels.

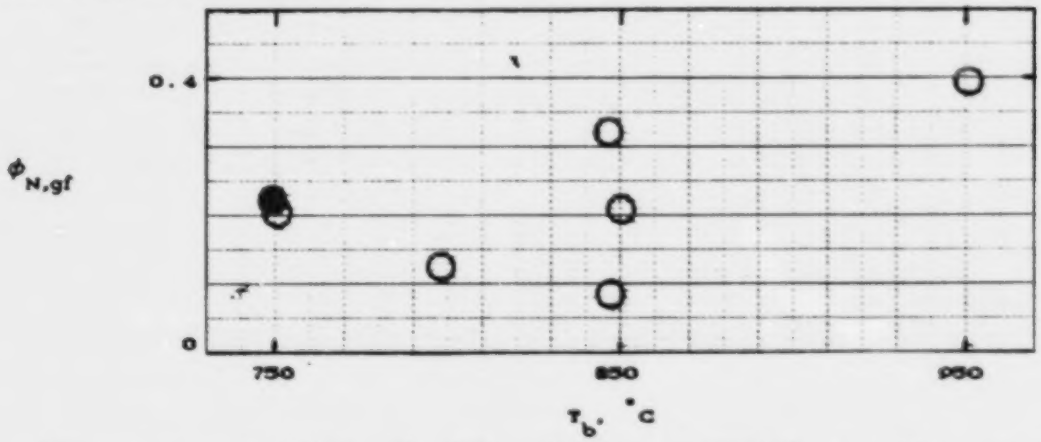

Fig. 7.2 Fraction of fuel nitrogen converted to NO_x versus bed temperature. Key to symbols in Fig 4.1.

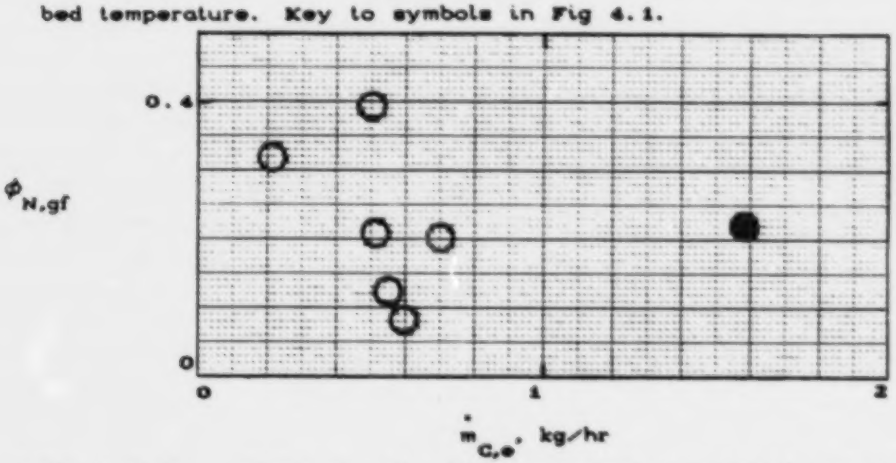

Fig. 7.3 Fraction of fuel nitrogen converted to NO_x versus the elutriated carbon flux. Key to symbols in Fig 4.1.

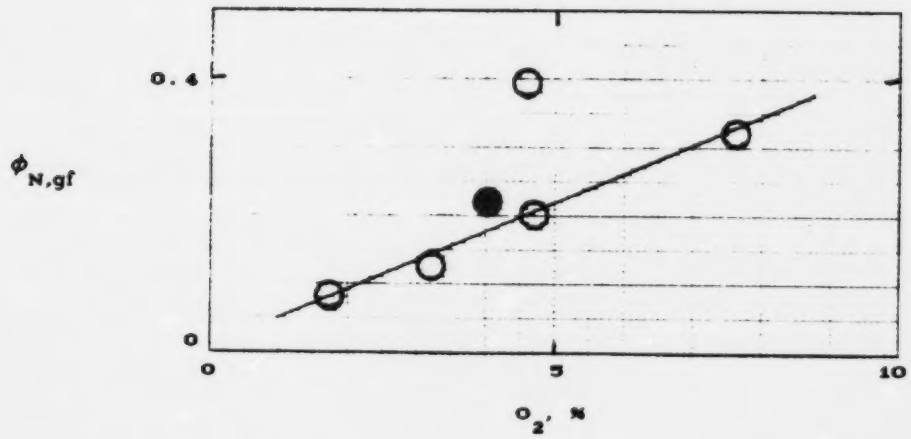

Fig. 7.4 Fraction of fuel nitrogen converted to NO_x as a function of stack gas oxygen concentration. Key to symbols in Fig. 4.1.

8. Carbon monoxide

Carbon monoxide levels in the exhaust gas, Figure 8.1, were in the range 0.01---0.06 % in all runs except one. The exceptional run was that at the lowest exhaust O_2 level, 1.7 % .

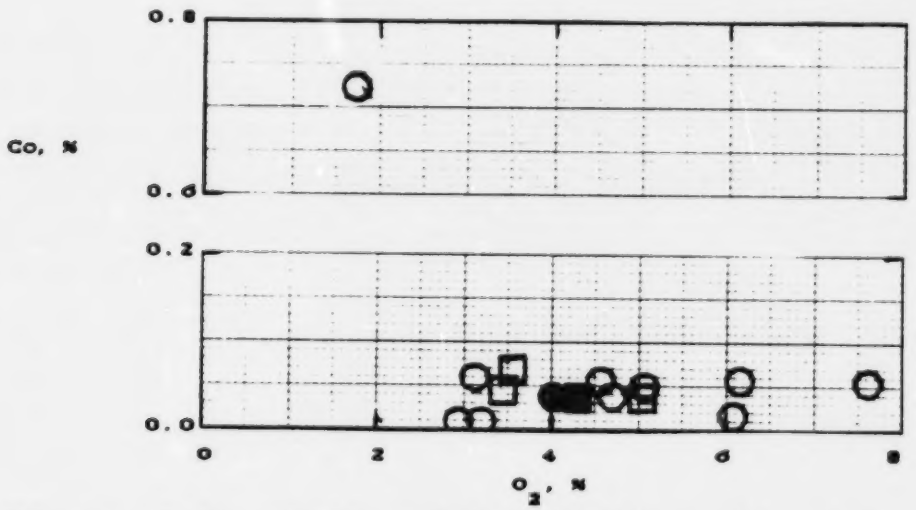

Fig. 8.1 Carbon monoxide content of the exhaust gases versus the oxygen content. Key to symbols in Fig. 4.1.

9. Comparision with other coals

9.1 Overhead carbon loss

In addition to Highvale coal, the performances of four coals from eastern Canada have been characterized using the present pilot plant. For each of the fuels the overhead carbon loss observed in trials using the underbed feed mode, in the 800---950 °C bed temperature range, has been correlated with the operating conditions using equation (2);

$$\phi_{C,of} = C_o \; v^{a_1} \; \phi_a^{a_2} \; e^{(a_3 r)} \; e^{(a_4/T_b)} \; \hat{D}_{p,s}^{a_5} \qquad (2)$$

Values of the resulting coefficients together with the free swelling index (FSI) of the fuels are listed in Table 9.1.

Table 9.1 Correlation of overhead carbon loss for the temperature range 800---950°C.

Fuel	C_o	a_1	a_2	a_3	a_4	a_5	FSI
Highvale*	2.60×10^{-6}	2.64	-5.27	-2.00	8490	****	0
Evans	2.06×10^{-3}	0.58	-0.71	-0.94	2833	-0.35	1.5
Minto-Devco	3.35×10^{-4}	0.86	-0.50	-0.36	5200	-0.74	5.0 5.5
Lingan	7.42×10^{-4}	-0.37	-2.46	-0.06	6109	0.65	7.0

* - $\hat{D}_{p,s}$ was not varied in this set. The coefficient a_3 was determined from trials at the 750 °C bed temperature level.

The operating conditions for the various fuels did not always allow for accurate prediction of all coefficients. For example, runs at low fluidizing velocity were unsuccessful, due to clinkering, when using the Lingan fuel. However, the

correlations adequately predict the $\phi_{C,of}$ within the range of operating conditions from which they are based.

Figure 9.1 shows the $\phi_{C,of}$ predicted by the different empirical correlations under typical operating conditions, as a function of free swelling index of the fuel. The following trends can be seen on $\phi_{C,of}$ with increasing fuel FSI :

- increasing overhead carbon loss
- reduced relative effect of cyclone product recycle

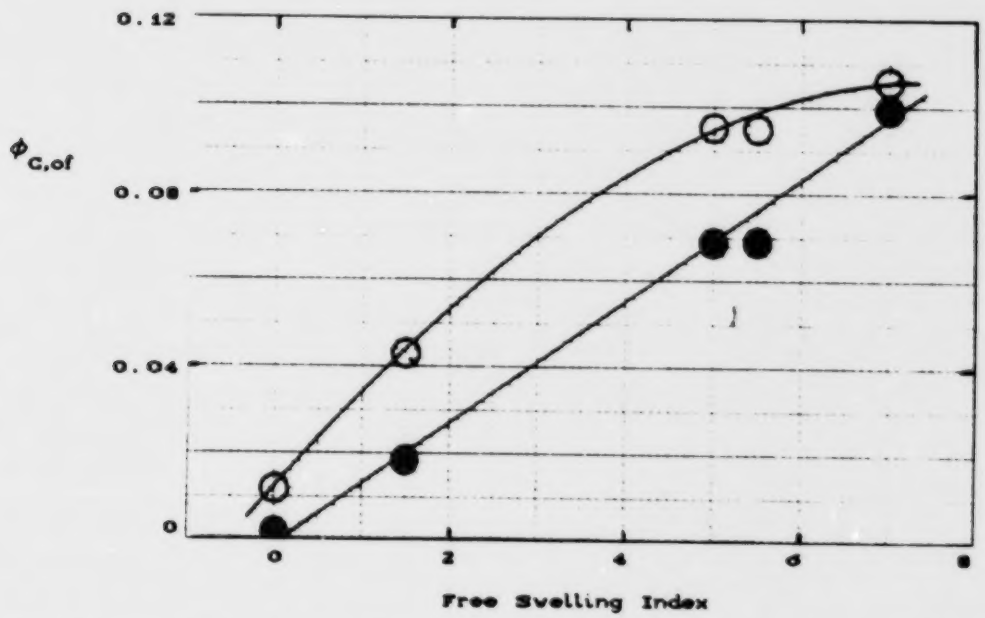

Fig. 9.1 Flux ratio of overhead carbon loss to carbon fed in the fuel predicted by empirical correlation versus fuel free swelling index. Operating conditions:

T_b =850 C°; v=2 m/s; ϕ_a =1.2; $\hat{D}_p$ =1.4 mm for stone used during the lingan trials and 0.5 mm for the others

Key to Symbol :

○ r = 0

● r = 0.9

Note: Coal particle diameter had an insignificant effect on combustion efficiency for the Eastern Canadian coals. In the Highvale trials only one lot of coal was used, with mean diameter 11 mm.

The earlier work on Minto, Devco, and Evans coal showed $\phi_{C,of}$ to be independant of fuel particle size. To explain this phenomenon, it was proposed that the bulk of elutriated carbon originated from the continual shedding of relatively unreactive carbonaceous matter during combustion of a fuel particle. In light of subsequent work studying the combustion of single coal particles in a bench scale system (Zhang et al, 1987), a more likely explanation puts the particle fragmentation, observed after the devolatilization stage of combustion, as a critical factor controlling the production of elutriable carbon particles.

Within this context, the trend of increasing overhead carbon loss with increasing free swelling index of the fuel can be easily surmised. Apparently, char particles originating from a strongly swelling fuel are more prone to particle fragmentation in the abrasive environment of the fluidized bed.

The reduced relative effect of cyclone product recycle on $\phi_{C,of}$ with increasing fuel FSI may again be due to differences in char friability, with highly friable chars tending to undergo further breakup and eventual loss to the baghouse product stream upon recycling. Alternatively, this trend may indicate an inherent lower reactivity of char particles originating from highly swelling fuels.

9.2 Sulphur capture

When operating in the underbed feed mode, the average percentage of sulphur captured by the fuel ash was about 90 % . This is comparable to the sulphur capture range of 85---100 % found in the earlier work, when operating at a 3.7 Ca/S ratio, and with sorbent particles in the optimum size

range.

Little else can be said by way of comparison, since the particle size distribution of the ash, and the distribution of calcium within the various size fractions, remain unknown.

10. Comparison with the ERL trials on Highvale coal

10.1 Background

Burning of Highvale coal has also been investigated at the Energy Research Laboratories of CANMET (Stover, Anthony, Desai and Friedrich, 1982) using a relatively small cylindrical pilot plant combustor. The combustion chamber was 0.24 m i.d. by 1.2 m high, surmounted by a 1.8 m high freeboard extention increasing in diameter through a conical transition piece to 0.6 m i.d.

The bed was of sand, $\hat{D}_p \cong 1$ mm , and had an expanded depth of 0.41 m . The fuel, $D_p \cong 1$ mm , was fed pneumatically into the bed at a point 0.1 m above the distributor plate. The bed was operated in semi-continuous fashion, without sand feed or bed product withdrawal, for periods ranging from 2 to 4 hours.

10.2 Overhead carbon loss

With the exception of one run, the overhead carbon loss was 0.3---2.5 % of the fuel carbon. The atypical run had a 4.5 % carbon loss. Figure 10.1 shows the fractional overhead carbon loss as a function of bed temperature for the ERL trials and ours. Only data from the trials using underbed feed and zero cyclone product recycle from the present work have been plotted, since these operating conditions were used in the ERL study. The

range of $\phi_{C,of}$ from both studies is quite similar for the higher temperature trials ($T_b \cong 850$ & 950 °C). At the low bed temperature level ($T_b \cong 750$ °C), the ERL results showed higher overhead carbon loss.

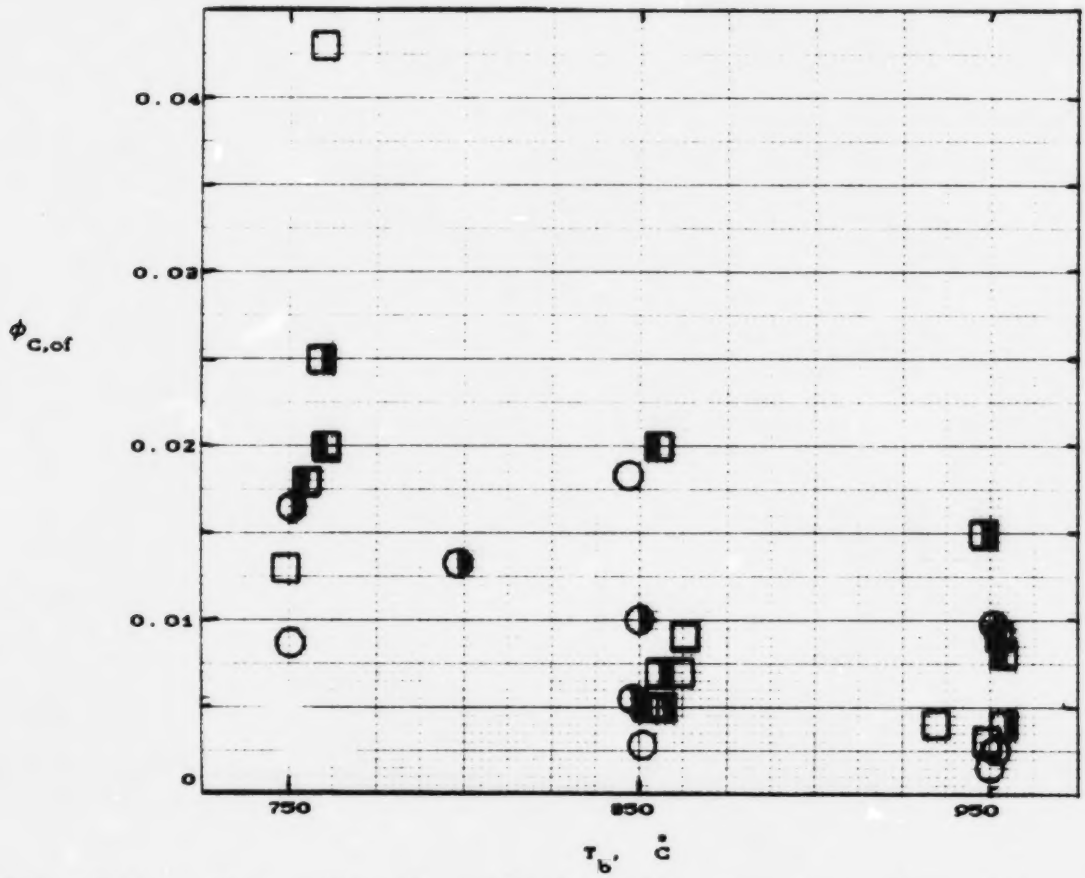

Fig 10.1 Flux ratio of overhead carbon loss to carbon fed in fuel as a function of bed temperature.

Key to symbols :

Reporter		v
○	- QFBC	1.1---1.5 m/s
◑	- QFBC	1.7---3.1 m/s
□	- ERL	1.2---1.3 m/s
◨	- ERL	2.2---2.5 m/s
◧	- ERL	3.7---4.2 m/s

An attempt to correlate $\phi_{C,of}$ with the operating conditions using the previously described empirical model (equation 3) indicated that bed temperature was the only significant variable. Regression analysis on this variable gave :

$$\phi_{C,of} = 5.6 \times 10^{-6} \; e^{(8400/T_b)} \qquad (4)$$

$$R^2 = 0.49, \text{ F ratio} = 15$$

This correlation and ours are in agreement as to the temperature effect, for the difference in the temperature factors, exp $(8400/T_b)$ and exp $(10500/T_b)$, is statistically insignificant.

Assuming that the form of equation 2 is adequate, the low explained variation about the mean of $\phi_{C,of}$ implies a high proportion of random error in the ERL data. The apparent lack of correlation with excess air or fluidizing velocity may be a consequence of the high random error, rather than an implication of high fuel reactivity suggested by the authors.

The high random error is not suprising, given the narrow range of overhead carbon loss. The smaller proportion of random error in our data is probably due to longer operating times and larger quantities of fuel consumed per test, reducing the effects of fuel variability and fluctuations in the operating conditions.

10.3 Sulphur capture

Figure 10.2 shows sulphur capture as a function of bed temperature for the ERL trials and ours. The ERL data show a

linear drop in sulphur capture with increasing bed temperature. This contrasts with our results which indicate a relatively flat response to bed temperature with a maximum at 850 °C. Although not clearly demonstrated in the literature, the markedly different effects of increased bed temperature on sulphur capture may be due to differences in the sorbent particle (in this case shale) size distributions.

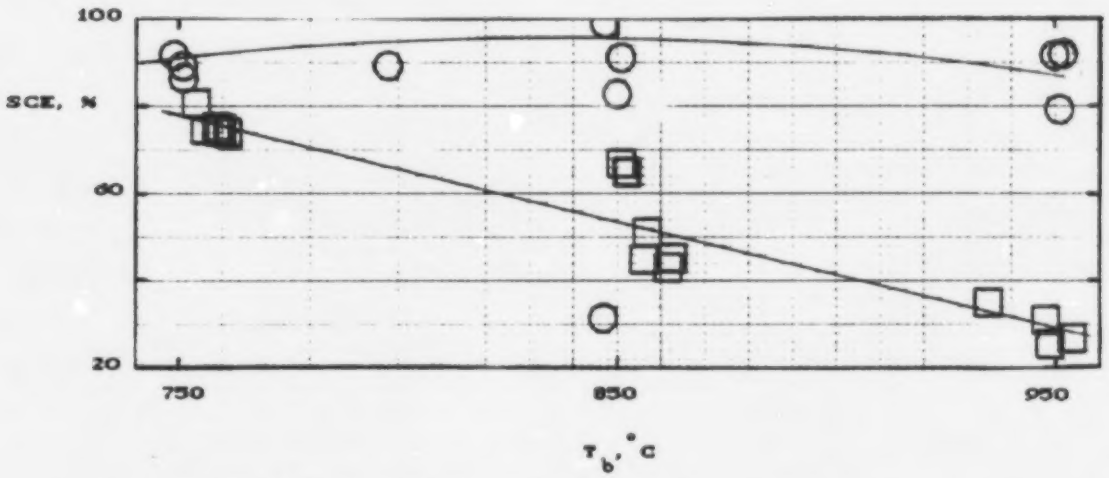

Fig. 10.2 Sulphur capture efficiency versus bed temperature.
Key to symbols :

○ - present work (based on gas analysis)

□ - reported by Stover et al (1981) (based on solids analysis)

Previous work on the performance of limestone as a sulphur sorbent in AFBC (Couturier, 1986) has indicated an optimum sorbent particle diameter range of 0.5---1.0 mm. Smaller particles tend to elutriate too readily and larger particles have a lower ultimate sulfation capacity.

The particle size distribution of sorbent particles occurring naturally in coal ash is largely determined by fuel preparation. During the ERL trials most of the fuel ash was

elutriated, since the bed depth remained constant without bed product removal. During our trials considerable accumulations of non-fluidizable shale particles were observed in the bed material. The fuel sizes used in the two studies apparently bound an optimum with respect to the resulting sorbent particle size distribution.

11. Conclusions

The present work demonstrates that Highvale coal can be burned with high efficency by AFBC at temperatures of 750---950 °C. By recycling a portion of the cyclone product, carbon burn-up efficencies higher than 99 % can be attained over the entire temperature range.

When using the underbed feed mode more than 80 % of the fuel sulphur was captured by the natural calcium compontent of the fuel ash over the temperature range studied. Virtually complete sulphur capture may be possible by judicious selection of fuel size.

The effect of overbed feeding of the fuel on carbon burn-up efficency was small, but using this feed mode resulted in lower sulphur capture at the 850 and 950 °C bed temperature levels.

For the sub-bituminous and bituminous coals studied to date, there is a strong correlation of overhead carbon loss with fuel free swelling index. Char particles originating from highly swelling fuels are apparently more prone to fragmentation and subsequent elutriation in the fluidized bed environment.

REFERENCES

Anthony, E.J., 1986, private communication, Energy Research Laboratories, Energy Mines and Resources Canada, CANMET, Ottawa

Becker, H.A. and Code, R.K. 1982, The Pilot Plant Installation at Queen's University for Studies of Atmospheric Fluidized Bed Combustion. Report QFBC.TR.82.1, Queen's Fluidized Bed Combustion Laboratory, Department of Chemical Engineering, Queen's University, Kingston, Canada K7L 3N6

Becker, H.A. and Code, R.K. 1983, Pilot Plant Trials on Atmospheric Fluidized Bed Combustion of High-Sulphur Eastern Canadian Coals (Minto and Devco) with Limestone Addition for Sulphur Capture. Report to Energy Mines and Resources Canada, CANMET, Ottawa. Report QFBC.TR.83.1, Queen's Fluidized Bed Combustion Laboratory, Department of Chemical Engineering, Queen's University, Kingston, Canada K7L 3N6

Becker, H.A., Code, R.K., McCleave, R.W., and Stephenson, J.R. 1985, Pilot Plant Studies of Fluidized Coal Combustion. Report to Energy Mines and Resources Canada, CANMET, Ottawa. Report QFBC.TR.85.1, Queen's Fluidized Bed Combustion Laboratory, Department of Chemical Engineering, Queen's University, Kingston, Canada K7L 3N6

Couturier, M.F. 1986, Sulphur Dioxide Removal in Fluidized Bed Combustors. Report to Energy Mines and Resources Canada, CANMET, Ottawa. Report QFBC.TR.86.1, Queen's Fluidized Bed Combustion Laboratory, Department of Chemical Engineering, Queen's University, Kingston, Canada K7L 3N6

Stover, N.S.H., Anthony, E.J., Desai, D.L. and Friedrich, F.D. 1981, Combustion Performance and Sulphur Capture During Fluid Bed Combustion of a Western Sub-Bituminous Coal and an Eastern Bituminous Coal. Report ERP/ERL 81-36 (J). Energy Mines and Resources Canada, CANMET, Ottawa.
Also issued as ASME paper 81-WA/FU-5, American Society of Mechanical Engineers, 345 E. 47 St., New York 10017

Zhang, J.Q.,Becker, H.A. and Code, R.K., 1987 Experimental Study on Devolatilization of Large Coal Particles in a Fluidized Bed. Proceedings of Ninth International Conference on Fluidized Bed Combustion, Boston, Massachusetts